BEAM LIFETIME EVALUATION BASED ON SIMULATION OF A VACUUM PRESSURE DISTRIBUTION FOR THE SPring-8-II COMMISSIONING STRATEGY THROUGH VACUUM CONDITIONING

Y. Ueda†, K. Tamura[1], H. Dewa, M. Masaki, T. Masuda, M. Oishi[1], H. Ota, M. Shoji[1], S. Takano[1], Y. Taniuchi, T. Watanabe[1]
Japan Synchrotron Radiation Research Institute (JASRI), Sayo, Hyogo, Japan
[1]also at RIKEN SPring-8 Center (RSC), Sayo, Hyogo, Japan

Abstract

SPring-8-II, a major upgrade of the third-generation light source SPring-8, aims to achieve low emittance below 100 pm·rad and to reduce the power consumption of the light source machine. The magnets in SPring-8-II feature narrow bore diameters for high magnetic fields, and are arranged with high packing factors. As a result, vacuum chambers along the entire storage ring are designed with narrow apertures, leading to low conductance, and space for vacuum components is limited. To overcome these constraints, we employ small-diameter stainless steel chambers and discrete compact photon absorbers. Non-Evaporable Getter (NEG) pumps are placed near photon absorbers to effectively evacuate photon stimulated desorption gas. We simulated the pressure distribution of the representative normal unit cell in SPring-8-II as a function of integrated beam dose considering the degradation of the pumping speed of the NEG pump due to gas sorption. On the basis of these results, we evaluated the beam lifetime evolution and formulated a preliminary commissioning strategy for increasing a stored current through systematic vacuum conditioning.

INTRODUCTION

The SPring-8-II project, a major upgrade of the third-generation light source SPring-8, has started in FY2024 [1, 2]. SPring-8-II is designed to achieve a beam emittance of less than 100 pm·rad and a stored beam current of 200 mA at an electron energy of 6 GeV. Simultaneously, the project aims for green facility operations by reducing power consumption to half that of the current SPring-8.

In SPring-8-II, multipole magnets for the high magnetic field gradients result in narrow bore diameters. To install vacuum chambers without the mechanical interference, we have adopted small-diameter, thin-walled stainless steel vacuum chambers. Furthermore, the magnets are arranged with high packing factors. Compact discrete photon absorbers [3] have been employed to protect the chamber walls from synchrotron radiation within the limited space. The small-diameter vacuum chambers result in the low conductance. Vacuum pumps are placed near the photon absorbers, which are the primary sources of photon-stimulated desorption (PSD) gas, thereby enhancing evacuation efficiency.

The pumping speed of the Non-Evaporable Getter (NEG) pumps, which are the main pump in SPring-8-II, saturates as gas sorption proceeds. Since this saturation leads to a stagnation of pressure improvement as operation progresses, restoring the pumping speed through NEG reactivation at appropriate intervals is essential for stable operation. In this study, we calculated the pressure distribution of the representative normal unit cell via Monte Carlo simulations and evaluated the beam lifetime before and after NEG reactivation at various integrated beam doses to provide a baseline for the commissioning strategy.

VACUUM SYSTEM

The storage ring of SPring-8-II consists of 48 unit cells. The normal cell accounts for 34 of 48 cells. Each normal cell, approximately 26 m long, comprises five bending sections (BSs) and six straight sections (SSs). Between the lowermost straight section (SS6) on the upstream cell and the uppermost straight section (SS1) on the downstream cell, a straight section is provided for the installation of insertion devices (IDs). The conceptual layout of a normal cell omitting the ID section is shown in Fig. 1.

Thirteen photon absorbers are installed in each normal cell. These include nine absorbers (ABs), two crotch absorbers (CRs) that have the extraction aperture of synchrotron radiation to the beamlines, and two bending chamber absorbers (BCAs) located at the downstream parts of BS2 and BS5. The photon absorber (AB/CR) features a radiation shielding structure that confines synchrotron radiation within itself to reduce scattered light toward the chamber walls [3, 4]. In contrast, the BCA adopts a simple geometry designed to reflect scattered light from its inclined plane toward the chamber walls. In straight sections where an ID is not initially installed, ID dummy chambers (IDDs) are placed. An AB (IDD_AB) is installed at the downstream end of the IDD. ABs, CRs, and IDD_AB are made of chromium-zirconium copper (CuCrZr) alloy. BCAs are made of oxygen-free copper (OFC).

Since photon absorbers are the primary sources of PSD gas, vacuum pumps are strategically located in their vicinity for the evacuation efficiency. Furthermore, vacuum pumps are installed at all five BS locations regardless of the presence of a BCA. The IDD, which is approximately 4 m long, has the evacuation chamber (IDD_Pump) equipped with a vacuum pump at the upstream end. The pumping system is a combination of NEG pump for evacuating active gases such as hydrogen (H_2) and carbon monoxide (CO), with sputter ion pump (SIP) of the noble diode (ND) type for evacuating gases not sorbed by the NEG, such as methane (CH_4) and noble gases.

† yueda@spring8.or.jp

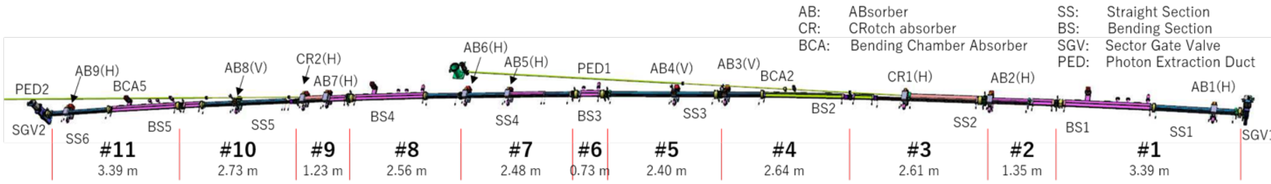

Figure 1: Chamber configuration of the normal cell of SPring-8-II (ID section omitted for clarity) [3].

SIMULATION OVERVIEW

In this study, the pressure distribution due to PSD gas was simulated using the software packages, SynRad+ and MolFlow+ [5]. These are Monte Carlo simulation tools developed by CERN for calculating photon flux distributions and pressure distributions, respectively. We imported the 3D geometry of the vacuum chambers of a complete normal unit cell (including the IDD section) into these software programs to evaluate these distributions in the SPring-8-II storage ring.

SynRad+ calculates the electron beam trajectory and the number of generated photons based on parameters such as beam energy, stored current, and the bending magnetic field distribution. The software outputs the photon flux distribution and the synchrotron radiation power distribution on the imported geometry.

MolFlow+ calculates the pressure distribution within the geometry based on the gas species (molecular mass), outgassing rates, and pumping speeds. By utilizing the same geometry as in SynRad+, the photon flux distribution can be imported into MolFlow+. The distribution of PSD gas at a specific integrated beam dose is determined by applying the PSD yield coefficient (η), which is defined as the number of molecules released per incident photon, and the elapsed time. The values of η in this simulation are derived from measured data at SPring-8 and reported values [6]. We calculated the pressure distributions induced by PSD gas corresponding to various integrated beam doses based on these parameters.

Simulation Conditions

In this SynRad+ simulation, the electron beam was assumed to be an ideal beam with zero emittance. The reflection ratio of photons on a surface of vacuum system depends on the material used for each component and the surface roughness. We used the default values in SynRad+ of iron (Fe) and copper (Cu) as proxies for the chamber sections (stainless steel equivalent) and the photon absorbers (CuCrZr and OFC), respectively.

We selected the following four gas species for the simulation; H_2, which has a high outgassing rate. CH_4, which is not evacuated by NEG pumps. CO and CO_2, which have a significant impact on beam lifetime due to their higher molecular mass. The simulations were conducted for four integrated beam doses and stored currents: 4 A·h at 50 mA, 10 A·h at 100 mA, 200 A·h at 200 mA, and 400 A·h at 200 mA.

The pumping speeds in this simulation are based on the specifications of SAES Getters' NEXTorr Z500 (NT-Z500-10ND, 5ND) and Z200 (NT-Z200-5ND), which combine a NEG cartridge with a SIP [7]. NT-Z500-10ND pumps are placed near photon absorbers with high gas desorption (AB2, AB3, AB4, AB6, CR2, AB9, IDD_AB), while NT-Z500-5ND pumps are installed near other absorbers and BSs. The compact NT-Z200-5ND is selected at BS2 due to the spatial constraints.

We simulated the pressure distribution based on two cases in this study. One case, called "after NEG Reactivation", is that the pumping speed remains equivalent to the condition immediately following NEG reactivation. Another case, called "before NEG Reactivation", is that the pumping speed of the NEG for CO and CO_2 decreases according to the amount of sorbed gas, which means the NEG pumps are operated continuously without reactivation after the initial activation. The pumping speeds for H_2 and CH_4 in both cases were assumed to be constant because the pumping speeds for these gas species show negligible degradation regardless of gas sorption.

The dependence of pumping speed on the amount of sorbed gas is shown in the brochure of NEG [7]. To estimate the gas load for each pump, we assumed that all gas desorbed from a photon absorber is sorbed by its nearest NEG pump. For the pumping speeds of pumps located where no absorbers are present (BS1, BS3, BS4, IDD_Pump), the "After NEG Reactivation" values were applied.

SIMULATION RESULT

We simulated the pressure distributions in the normal unit cell at four integrated beam doses. As an example, the pressure distributions for the two cases at a integrated beam dose of 200 A·h are shown in Figs. 2 and 3. The average pressures in the normal unit cell before and after NEG reactivation are summarized in Table 1.

In Fig. 2, the pressure becomes lower near the pumps and higher as the distance from the pumps increases. Regarding gas species, the pressure of H_2, which has the highest outgassing rate, is the highest, followed by CO, CO_2, and CH_4. CH_4, which has a lower outgassing rate but is not evacuated by NEG pumps, shows a relatively gradual distribution throughout the cell.

In Fig. 3, the pressure of CO exceeds that of H_2. The pressure of CO_2 increases. This trend is attributed to the fact that the pumping speeds for H_2 and CH_4 do not decrease, while those for CO and CO_2 decrease corresponding to the gas sorption. The pressure drop near the pumps becomes less for both CO and CO_2.

We evaluated the beam lifetime by applying the simulated pressure distribution of the normal unit cell to the entire ring as a representative model. The beam lifetime is determined by the gas scattering lifetime and the Touschek lifetime. The gas scattering lifetime accounts for the Rutherford scattering, the Møller scattering, and the bremsstrahlung. The Touschek lifetime is assumed to be 10 hours at 200 mA in 1920 bunches (equivalent to 0.1 mA/bunch). Fig. 4 shows the dependence of the product of stored current and beam lifetime (I·τ) on the integrated beam dose before and after NEG reactivation based on the simulated pressure distributions. In the plot, black dots represent I·τ before NEG reactivation, while red dots represent I·τ after NEG reactivation. The black and dashed red lines represent power-law fits to these data points. The gap between the two cases becomes wider at higher doses. The difference in I·τ is approximately a factor of three at 400 A·h. In terms of gas scattering lifetime, these are 17 hours and 52 hours, respectively.

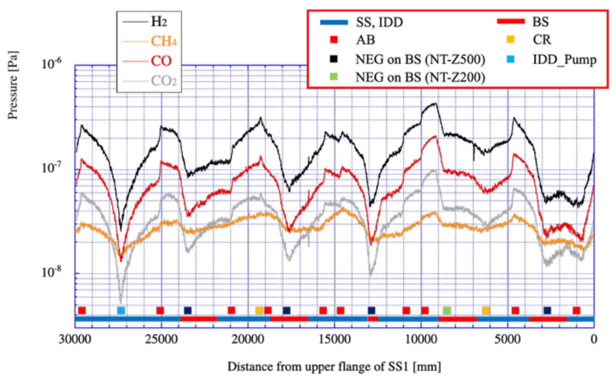

Figure 2: Pressure distribution of PSD gas at 200 A·h, 200 mA in the normal unit cell after NEG reactivation.

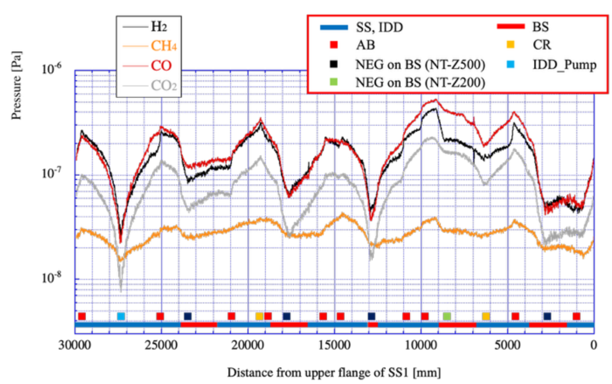

Figure 3: Pressure distributions of PSD gas at 200 A·h, 200 mA in the normal unit cell before NEG reactivation.

Table 1: Average Pressure at 200 A·h

Gas Species	Ave. pressure [Pa]: After NEG reactiv.	Ave. pressure [Pa]: Before NEG reactiv.
H_2	1.6e-7	1.6e-7
CH_4	2.8e-8	2.8e-8
CO	7.4e-8	1.9e-7
CO_2	3.6e-8	8.5e-8
Total	3.0e-7	4.6e-7

Table 2 shows the projected evolution of the beam lifetime from the start of commissioning based on the I·τ fitting before NEG reactivation. In this operation, the stored current was determined solely by the assumption that it increases only up to a value maintaining a peak pressure of less than 5×10^{-5} Pa within the normal unit cell. The conditioning time is assumed to be 12 hours per day. Under these conditions, the integrated beam dose on day 83 reaches 163 A·h. At this dose, the gas scattering lifetime becomes 11.7 hours, which results in a beam lifetime of 5.4 hours before NEG reactivation. After the NEG reactivation, the gas scattering and beam lifetimes increase to 28.7 and 7.4 hours, respectively.

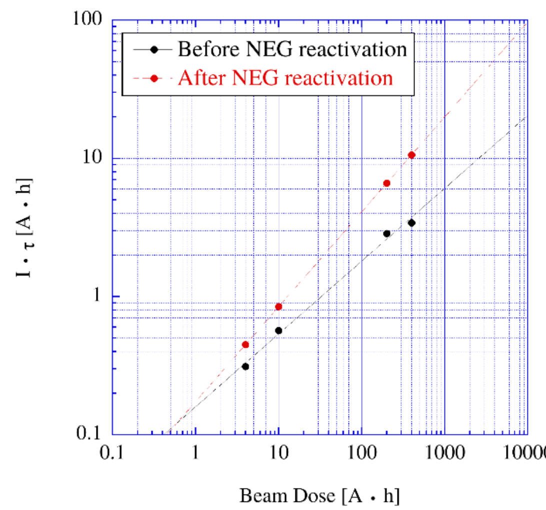

Figure 4: Comparison of I·τ distribution and data fitting before and after NEG reactivation.

Table 2: Beam Lifetime Evolution

Elap. Day	Stored current [mA]	Beam Dose [A·h]	Beam lifetime [hr.]
1	1	0	11.9
5	20	2.2e-1	3.3
9	50	1.2	3.2
14	100	4.9	3.1
18	150	9.7	2.8
22	200	17	2.6
83	200	163	5.4

CONCLUSION

We simulated the pressure distribution of various gas species in the representative normal unit cell of SPring-8-II at various integrated beam doses for the two cases, “before NEG reactivation” and “after NEG reactivation”. The preliminary beam lifetime evaluation based on the normal unit cell pressure distributions suggests a promising outlook where the stored current reaches 200 mA within a month, and the beam lifetime reaches 5.4 and 7.4 hours before and after NEG reactivation after three months of operation, respectively. Future work will involve simulating the pressure distribution in other parts of the storage ring such as the four long straight sections with or without damping wigglers [8]. We will develop a comprehensive commissioning strategy by integrating these results and the radiation dose assessments.

REFERENCES

[1] T. Watanabe and H. Tanaka, "SPring-8 Upgrade Project: Accelerator Redesigned and Restarted", *Synchrotron Radiat. News*, vol.36 (2023) issue 1, pp. 3-6. doi:10.1080/08940886.2023.2186117

[2] H. Tanaka *et al.,* "Green upgrading of SPring-8 to produce stable, ultrabrilliant hard X-ray beams", *J. Synchrotron Radiat.*, vol. 31 (2024) pp.1420-1437. doi:10.1107/S1600577524008348

[3] K. Tamura *et al.*, "Verification of SPring-8-II vacuum system prototype chamber", in *Proc. MEDSI2025*, Lund, Sweden, Sep. 2025, pp. 409-412. doi:10.18429/JACoW-MEDSI2025-THP59

[4] H. Dewa *et al.*, "Design of photon absorbers for the SPring-8-II vacuum system", presented at IPAC'26, Deauville, France, May 2026, paper TUP7689, this conference.

[5] MolFlow+ and SynRad+ , https://molflow.docs.cern.ch

[6] Y. Ueda *et al.*, "Beam lifetime evaluation based on simulation of a vacuum pressure distribution for the SPring-8-II storage ring", in *Proc. PASJ2025*, Tokyo, Japan, Aug. 2025, pp. 739-743.

[7] NEXTorr D/Z (UHV), https://www.saesgetters.com/highvacuum/solution/nextorr-d-z-uhv

[8] K. Tsubota *et al.*, "Design of a damping wiggler at SPring-8-II as a high-energy X-ray source", in *Proc. MEDSI2025*, Lund, Sweden, Sep. 2025, pp. 193-196. doi:10.18429/JACoW-MEDSI2025